Advance Publication Cover Page

Electrochemical Determination of CdS Band Edges and Semiconducting Parameters

Somaieh Miandari, Majid Jafarian,* Mohammad Ghasem Mahjani, Fereydoon Gobal, and Ashraf Heidaripour

Advance Publication on the web February 3, 2015 by J-STAGE
doi:10.1246/bcsj.20140393

BCSJ Revised December 2014
The Chemical Society of Japan

Electrochemical determination of CdS band edges and semiconducting parameters

Somaieh Miandari,[1] Majid Jafarian*,[1] Mohammad Ghasem Mahjani,[1] Fereydoon Gobal,[2] and Ashraf Heidaripour[1]

[1]Department of chemistry, K.N. Toosi University of Technology, P.O. Box 15875–4416, Tehran, Iran

[2]Department of chemistry, Sharif University of Technology, P.O. Box 11155-3516, Tehran, Iran

Received: 16-Dec-2014; E-mail: mjafarian@kntu.ac.ir (M. Jafarian)

Abstract

Cadmium sulfide (CdS) thin film was electrodeposited on indium tin oxide (*ITO*) under chronoamperometry technique. The SEM images showed that the hexagonal sheets of CdS deposited on the ITO surface. The X-ray diffraction (*XRD*) analysis confirmed this structure for CdS crystals and the average of crystalline size and the lattice constant parameters are approximately 39.54 and *a*=0.4136, c=0.6696 nm respectively. Photo-electrochemical investigations were performed by cyclic voltammetry (*CV*), linear sweep voltammetry (*LSV*) and electrochemical impedance spectroscopy (*EIS*) techniques. CdS band edges and density of states (*DOS*) were determined by *CV* technique. The band gap energy (E_{bg}) was measured by ultraviolet-visible (UV-Vis) spectroscopy and electrochemical methods. Mott-Schottky plots were used to find the values of flat band potential (E_{fb}), donor density (N_D) and Debye length (L_D). Also, the position of surface states was investigated

by Mott-Schottky and *LSV* techniques. *EIS* was employed to confirm our electrochemical findings and investigate the charge transfer mechanism.

Keywords: band edges, cyclic voltammetry, impedance spectroscopy, DOS, Mott-Schottky

1. Introduction

The use of photo-electrochemical cells is receiving widespread attention to mediate the direct conversion of optical energy to electricity. N-type semiconductors as photo-anodes have a key role in improving the efficiency of solar cells[1, 2]. Among various n-type semiconductor materials, Cadmium sulfide (CdS) has increasingly attracted interest because of its superior optical, photoluminescence, photosensitization and photocatalytic properties[3]. CdS thin film has many potential applications in various optoelectronic devices[4, 5] with a wide direct optical band gap of 2.4eV [6, 7]. So far several studies have been performed on the electro-deposition of CdS and considerable effort has been focused on the investigation of its photo-properties by several methods such as photoelectron and tunneling spectroscopy[8]. Semiconductors were mostly investigated by physical methods while electrochemical methods could help as a complementary method to study electron transferring behavior and the positions of the energy levels in the actual systems (at the interface of a semiconductor-electrolyte). It seems that usage of electrochemical technique is an acceptable method instead of ultraviolet-visible (UV-Vis) spectroscopy and the extracted information is comparable in two methods. Varying the applied potential (as a function of energy) into the electroactive species leads to transfer electrons just as the changing the UV-Vis wavelength which results to transit electrons. Recently, the usage of electrochemical methods such as cyclic voltammetry (*CV*) has been widely used for the quantitative estimation of the position of band energy and surface states of various semiconductors in suitable electrolytes[9-13]. Rengaraj and co-workers[3] studied microspheres

of CdS on glassy carbon electrode (GCE/CdS) and showed that a decrease in the band gap energy (E_{bg}) results a decrease in the electron transfer resistance of GCE/CdS. Inamdar et al.[8] reported a direct correlation between the electrochemical band gap and the electronic spectra of CdS nanoparticles in DMF. Also Nesheva and co-workers[14] determined density of states (*DOS*) in amorphous CdS and In/CdS films from space charge-limited current measurements on isotype CdS-Si heterojunctions. In addition, most previous works employ electrochemical impedance spectroscopy *(EIS)* and Mott-Schottky methods to reveal the mechanism of charge transfer and the values of flat band potential (E_{fb}), space charge capacitance (C_{sc}), the chemical capacitance[15] as a function of the change of electrons number and N_D parameters which are necessary to characterize semiconductor-electrolyte junctions[16-19]. Our research group has published the results of photo-electrochemical studies by *EIS* technique on electrodeposited n-type PbS[20, 21]. To the best of our knowledge no work has been done on the determination of DOS and a few studies have been reported on the investigations of the photo-properties (band gap, energy diagram etc.) for CdS by electrochemical methods in alkaline solution.

So, the importance of improved methods as mentioned above, make us to determine the position of conduction band (*CB*), valence band (*VB*) and surface states to investigate the photo-properties, semiconductor parameters (such as E_{fb}, E_{bg}, donors density (N_D) and Debye length (L_D)) and charge transfer mechanism of electrodeposited CdS thin film in the alkaline electrolyte by means of UV-Vis spectroscopy and several electrochemical methods e.g. *EIS*, *CV*, linear sweep voltammetry (*LSV*).

2. Experimental

2.1. Materials

$Cd(NO_3)_2$, $CS(NH_2)_2$, NaOH used in this work were Merck products of analytical grade and used without further purifications. Doubly distilled water was used throughout.

2.2. Preparation of ITO/CdS electrode

Indium tin oxide (ITO) sheet with the area of $1cm^2$ was cleaned thoroughly with doubly distilled water, acetone, ethanol and sonicated in isopropanol prior of CdS electroplating and used as the working electrode. Chronoamperometry was used to electrodeposit cadmium and subsequently sulfur for 1 min each. In the potentiostat process, the applied potentials were selected from the related *CV* plots in the suitable media. First, Cd was electrodeposited on ITO from a 0.1M solution of $Cd(NO_3)_2$ at -0.9V/SCE. Subsequently, S^{2-} anions were oxidized onto the Cd surface from an alkaline solution (pH>13) containing 0.2 M thiourea at -0.67V/SCE. After electrodepositing of each layer the surface of the electrode was rinsed with distilled water to remove unabsorbed ions. The under potential deposition (*UPD*) procedures mentioned above were repeated 10 times to achieve 10 layers of CdS. The resulting electrode is denoted as ITO/CdS.

2.3. Instruments and techniques

All electrochemical measurements were carried out in a conventional three electrode cell powered by an electrochemical system comprising of EG&G model 273 potentiostat/galvanostat and model 1025 frequency response analyzer run by a PC through M270 and M398 commercial softwares via a GPIB interface. The frequency range of 100kHz to 10mHz and modulation amplitude 5mV were employed in *EIS* studies. A saturated calomel electrode (SCE), a graphite rod and the ITO/CdS electrode were used as the reference, counter and working electrodes respectively. The impedance studies were carried out at various potentials. The analysis of experimental impedance data was performed by Zview 3.1 software. The capacitance measurements were carried out at 1000Hz by sweeping the potential from 1 to -1.5V/SCE with 50mV/s to generate the Mott-Schottky plots. UV–Vis spectroscopic investigations were performed using Perkin Elmer model Lambda 25 double beam spectrophotometer in the range of 200-800nm. It is important to mention that the substrate effect was eliminated by setting the ITO as a substrate. Then the obtained UV-Vis spectrum

is related to the CdS film. The grazing method was used to record the X-ray diffraction (XRD) spectrum of CdS thin film by a system of PANalytical company (model X'Pert Pro MPD) with graphite monochromatized Cu-K_α radiation (λ=0.154 nm). This instrument works with voltage and current setting of 40 kV and 40 mA respectively, employing scanning rate of 0.04 deg/min in 2θ range from 20 to 85°. The image of scanning electron microscope (SEM) was obtained by Seron technology company microscope (model AIS2100) with accelerating voltages of 0.5-30 kV. Also it was used field emission scanning electron microscope (FE-SEM), model HITACHI S-4160, with accelerating maximum voltage 30kV for the better resolution of the image of deposited film. A 100W tungsten lamp was used in photo-electrochemical works. All studies were carried out at 298±2K.

3. Results and Discussion

3.1. X-ray diffraction analysis of CdS

XRD pattern in figure 1 corresponded with the JCPDS database no. 01-080-0006 for hexagonal CdS[22]. The strong and sharp peaks confirm that deposited thin film on ITO is related to the high crystalline CdS[23]. The average crystalline size was determined from the half-width of the diffraction major peaks using Debye–Scherrer's formula[24]:

$$D = k\lambda / \beta\cos\theta \tag{1}$$

where λ is the wavelength of Cu-Kα radiation (0.15406 nm), θ the angle of the diffraction peak, D the average crystallite size, k the geometric factor, and β the full width at half maximum (FWHM) in radian unit. The average crystalline size was calculated approximately 39.54 nm. Also the broadness of the peaks indicates that the product is nanocrystallized[25]. The plan spacing d_{hkl} of the individual lattice planes are obtained from the quadratic Bragg equation is obtained:

$$d_{hkl} = \frac{\lambda}{2\sin\theta} \tag{2}$$

The value of d_{hkl} was determined 0.238 nm. Then the lattice constant parameters with the indices (*hkl*) were calculated from the equation of plane spacing for the hexagonal crystal system and Bragg's law for diffraction as follow[26]:

$$\sin^2\theta = \frac{\lambda^2}{4}\left[\frac{4}{3}\left(\frac{h^2+hk+k^2}{a^2}\right)+\frac{l^2}{c^2}\right] (a, c= \text{lattice constants}) \quad (3)$$

where *h, k, l* are the lattice planes and *d* is the inter planar spacing. The calculated lattice constants of CdS were *a*=0.4136, c=0.6696 nm, which were very close to that of the JCPDS database no. 01-080-0006[22].

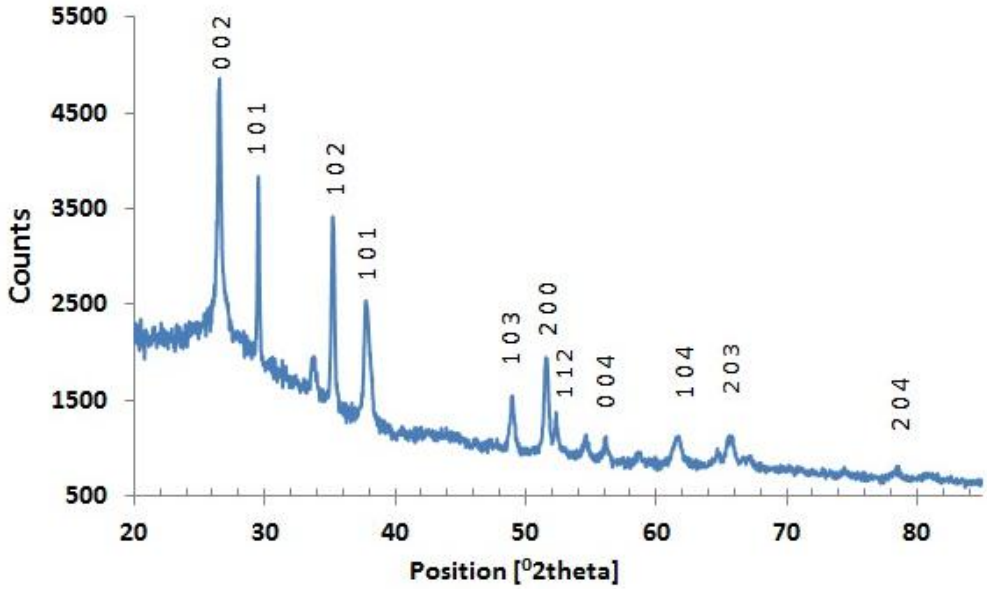

Figure 1. X–ray diffraction patterns of the CdS film deposited on ITO substrate.

3.2. SEM images of CdS

Figure 2 shows SEM and FE-SEM images of electrodeposited CdS thin film on ITO as substrate. Generally CdS film is seen composed of several nanosheets with a hexagonal structure mostly cross each other, figure 2a. As the surface of CdS film look likes Echeveria leaves (one type of cactus) in which each sheet grows from different centers. The FE-SEM images with high resolution show the thickness of each sheet is approximately uniform (about 100 nm) and the typical size of sheets is between 500nm to 2μm (figure2b). Also, each nanosheet composes of enormous CdS nanoparticles with uniform size of 30nm zoomed in figure 2c. The presence of nanoparticles and large area of

electro-deposited CdS film promote the internal trapping of light by scattering (redirecting) the light in the film and also improve the transport of charge carriers through the CdS thin film[27, 28]. So the efficiency of light absorption increases with respect to that of the dense and homogenous films.

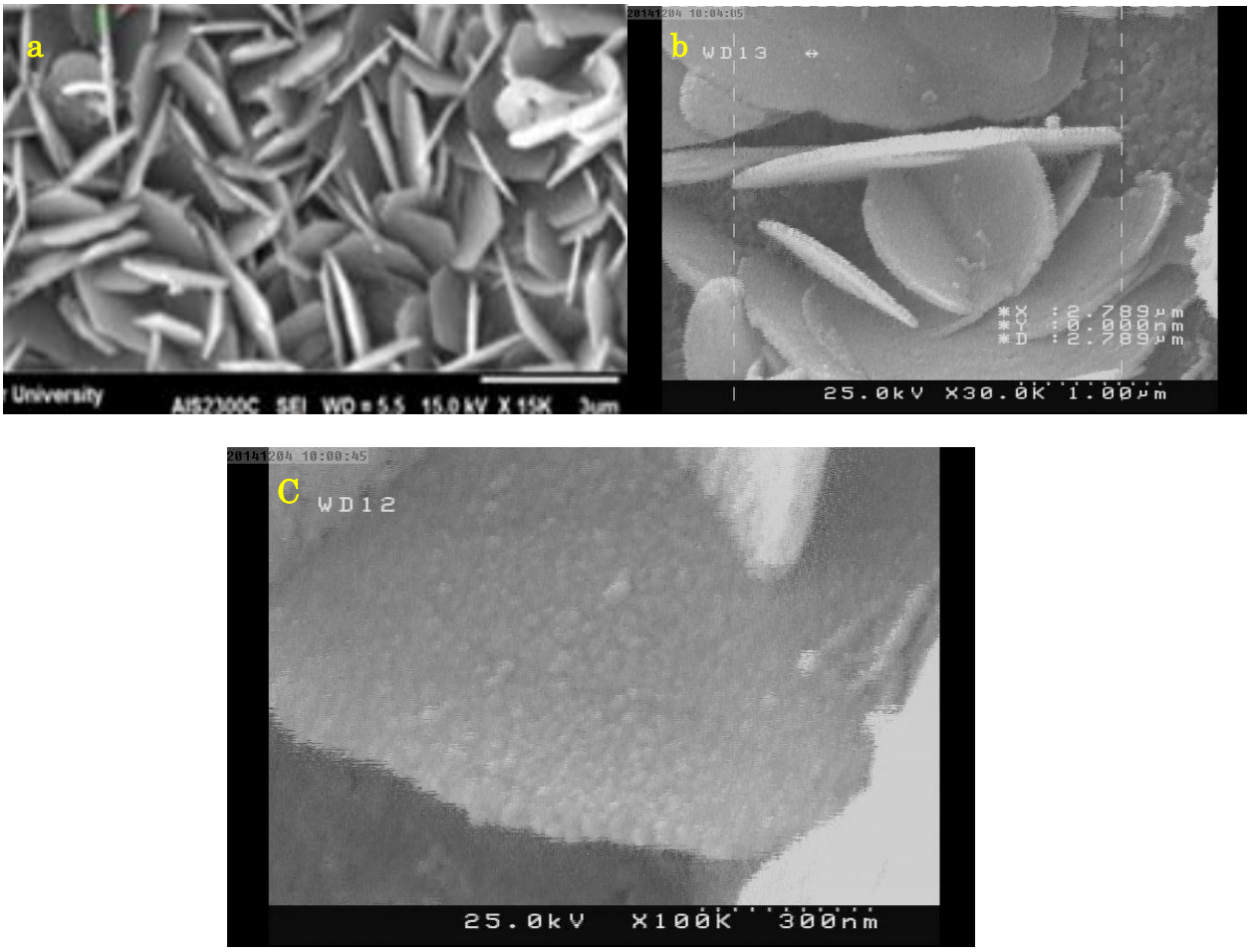

Figure 2. a) SEM, b and c) FE-SEM images of electrodeposited CdS film on ITO substrate.

3.3. UV-Vis Studies

Figure 3a presents the UV-Vis spectrum of ITO/CdS in the range of wavelength (λ) from 300 to 800nm. The band gap of CdS is about 2.4eV[7] which is approximately accordance to absorbance wavelength 518nm. So it is expected that absorbance edge initiates at 518nm while according to figure 3a the absorbance occurs over 518nm (near infrared absorption). A red shift in the absorbance edge or decrease in the band gap value of CdS could be referred to light scattering in the film or

increase in the spectra-trapped charge carriers[29]. In many amorphous semiconductors, near the band edge, the absorption coefficient α shows an exponential dependence on photon energy usually obeying Urbach's empirical relation[30] as:

$$\alpha_{(\upsilon)} h\upsilon = A^{*}(h\upsilon - E_{bg})^{1/n} \quad (4)$$

where A^{*}, h and $h\upsilon$ are a constant value, Plank's constant and incident photon energy (E) respectively, and n is a number that features the transition process. For the allowed direct transitions the coefficient n is equal to 1/2 and for indirect allowed transitions n= 2[31]. Also $\alpha(\upsilon)$ is the absorption coefficient defined by the Beer-Lambert's law as $\alpha = 2.3A/d$ [30], where d and A are thickness of film absorbance of light, respectively[31]. So the band gap of CdS can be determined from a fitted straight line of plotting $(ah\upsilon)^2$ versus E plot (figure 3b). The E_{bg} value was obtained 2.25 eV for the CdS film.

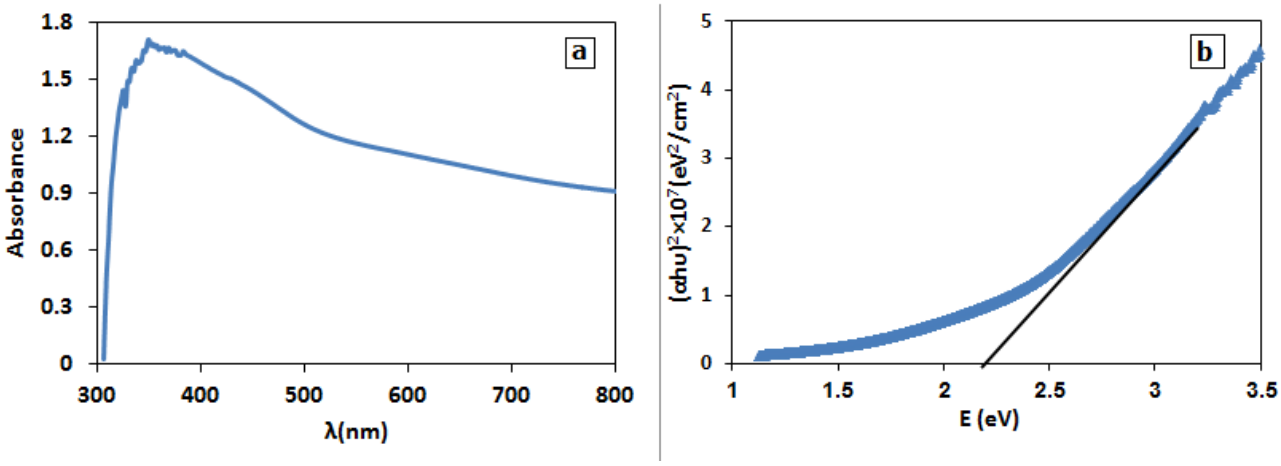

Figure 3. UV-Vis absorption spectrum a) and $(\alpha h\upsilon)^2$ *vs. E* curve b) for CdS thin film on ITO.

3.4. Cyclic Voltammetry Measurements

Figure 4 presents the *CV's* of ITO and ITO/CdS at a potential sweep rate (*S.R*) of 100mV/s in 0.1M NaOH solution in the dark and under illumination (D&I) conditions. For ITO in the *CV* diagram oxidation and reduction of water occurs at +1.2 and -1.6V/SCE and a small broad peak

appear at -0.9V/SCE (with edge located at -0.75V/SCE) in the cathodic branch of the voltammogram. This small broad peak is attributed to reduction of ITO material like SnO_2. Since the water oxidation potential lies slightly above the *VB* edge of ITO and the reduction potential of alkaline solution (-1V/SCE at pH=13) places at or slightly below the edge of *ITO CB*, so it could be concluded that the cathodic onset potential is attributed to the location of *CB* of ITO and the edge of *VB* is not measurable in alkaline solution. While the *CB* and *VB* edges of CdS could be determined in alkaline solution because its *VB* potential is more negative than that ITO [32, 33]. The electrochemical study of CdS as witness in the voltammograms in the D&I conditions more dramatic features. Higher currents and small shifts in the anodic side of the voltammogram is in good accordance to n-type nature of CdS and enrichment of the *VB* with holes upon illumination [32]. The reduction peak related to hydrogen evolution which occurs at -1.2V/SCE in the dark condition shifts to -1.4V/SCE under illumination with higher value of current density. In addition the anodic shift is observed in the oxidation peak at -0.6V/SCE in the dark toward -0.4V/SCE under illumination condition. This is because of some surface/adsorbate states "spread" below where in the dark are largely filled and under illumination are mostly vacant. Accordance to the *CV* diagram of ITO/CdS in alkaline solution the position of the *VB* and *CB* seems to be at around 1.2 and -1.1V/SCE. These findings set the band gap about 2.3eV and the donor state at the lower -0.3 eV below the *CB* in alkaline solution. So the electrochemical finding is in fair agreement with our optical findings (2.25eV) and good agreement with the literatures[6, 7].

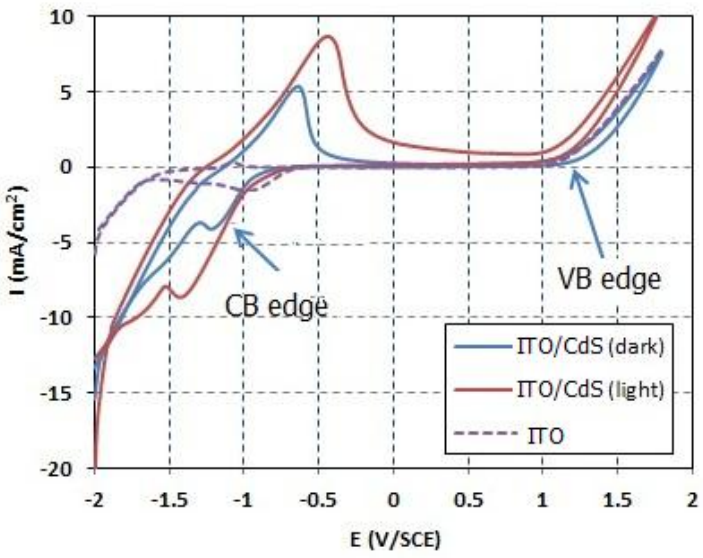

Figure 4. Cyclic voltammograms of ITO and ITO/CdS samples in 0.1 M NaOH solution under dark and illumination conditions, S.R=100 mV/s.

Figures 5a&b illustrate the chemical capacitance and the total charge density plots versus potential. These diagrams were extracted from cyclic voltammograms. As reported[11], it is assumed that the rate of electron transfer between thin film and electrolyte is negligible. In such conditions, capacitance could be calculated via equation 5 because the electrode response is a criterion of its capacitance, $C_\mu = dq/dE$, so:

$$i = dq/dt = \nu C_\mu \tag{5}$$

where i is the average cathodic and anodic current densities (A.cm^{-2}) at the same potential, C_μ chemical capacitance, v scan rate and q is the charge density. Since the film capacity, related to electron accumulation in the semiconductor, is as a function of the electrode potential, then the *CVs* would be informative about capacities. In addition, electron population *n(E)* as a function of film potential could be determined by *CV* so that change of electron *dn* is a direct function of *i dE*.:

$$i = -e_\circ \frac{dn}{dt} = -e_\circ \nu \frac{dn}{dE}\,;\; dn = -\frac{idE}{e_\circ \nu} \tag{6}$$

where $e_\circ$ is the charge of electron. This method [34] monitors the current injected into the film as the potential is scanned[35]. Hence, *dn* is *a function of DOS*; i.e. more DOS leads to high *dn*. *DOS* is

calculated by multiplying each value of capacitance by the potential so it could be determined by the *CV* method at any potential. The current density or charge distribution (in figure 5b) changes exponentially with potential, i.e. current increases highly at potential more negative than -1.1V/SCE. This exponential increase in current is in good agreement with equation 7 because *i* is a function of *C* and *C* is an exponential function of *E*:

$$C_{sc} = \varepsilon\varepsilon_{\circ} / L_D \cosh[e(E - E_{fb})/kT)] \quad (7)$$

This equation indicates when *E* is more negative than E_{fb} the electron density at the surface becomes more than that of in the bulk. This range of potential corresponds to the accumulation region, in which C_{sc} rises exponentially with cathodic increase in *E*[32]. Also, the electronic conductivity depends on the density of electrons in the *CB*[36].

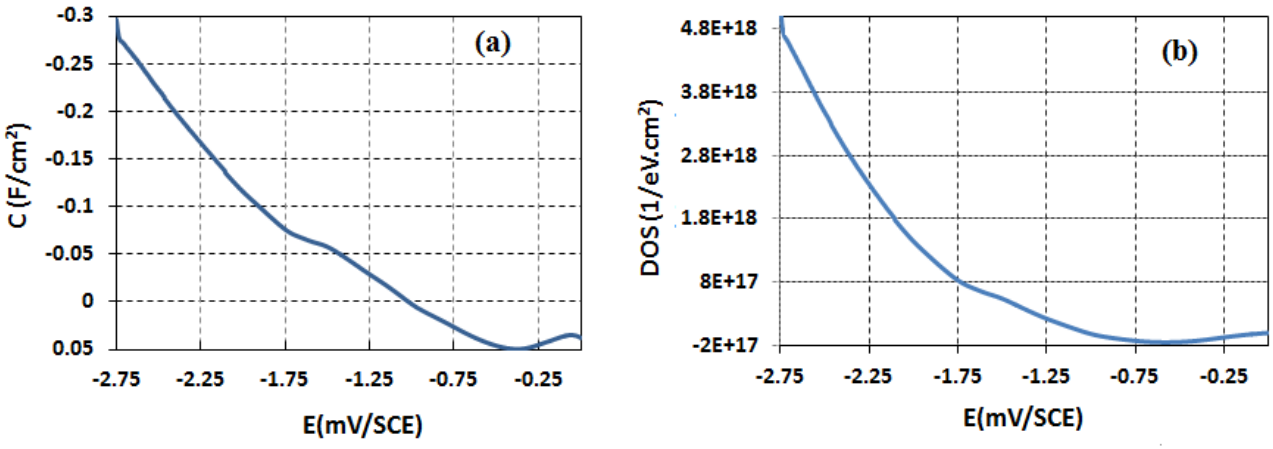

Figure 5. (a) Capacitance vs. Potential and (b) DOS plots of CdS thin film in the 0.1M NaOH solution.

3.5. LSV and determination of surface states

LSV diagrams of ITO/CdS thin film are plotted between ranges from -0.8 to 0 V/SCE in 0.1 M NaOH solution (figure 6a). It is used for characterizing of semiconductor type and determining the position of E_{fb}. These diagrams show that the E_{fb} is at around -0.8 V/SCE where in which cathodic currents abruptly increase in D&I conditions. At this potential, electrons flow from the *CB* to H_2O and produce H_2 at the electrode surface. At potentials more positive than E_{fb} cathodic current is seen

while under illumination, the anodic current is observed. This difference is due to increase of hole carriers in the *VB* under illumination. This behavior is accordance with the n-type nature of CdS[32]. The maximum of photocurrent is obtained about 30μAcm^{-2}. Existence of a shoulder at around -0.7V/SCE in D&I condition which is zoomed and shown in figure 6b, is a kind of the capacitance behavior related to surface states and/or traps. The capacitance behavior is a kind of charging or discharging phenomena by electrons which is seen as an abrupt change in current independent of potential. The difference of current density at -0.698V/SCE is about 7μA.cm^{-2}, figure 6b. So the value of capacitance is calculated 7×10^{-5} F.cm^{-2} by using the equation 5 which is close to expecting the value of Helmholtz double layer C_H in the surface state. In addition, the value of stored charges in the surface states Q_{ss} is obtained 2.1×10^{-7} C.cm^{-2} using equation 6.

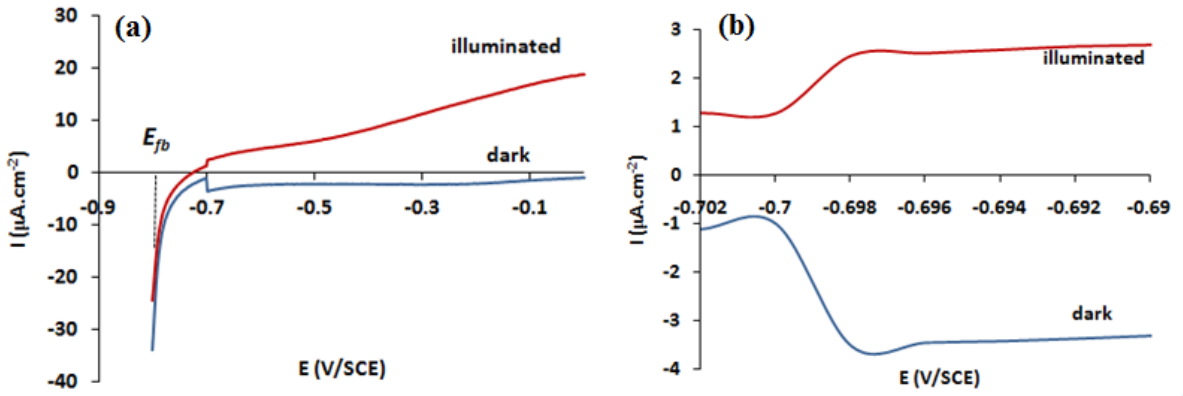

Figure 6. (a) Original and (b) zoomed linear sweep voltamograms of ITO/CdS electrode in the 0.1 M NaOH solution in dark and illumination, S.R= 100 mV/s.

3.6. Capacitance Measurements and Semiconducting Properties of CdS Film

A space charge layer is formed inside the ITO/CdS thin film in contact with a solution 0.1M NaOH. The capacity and thickness of the space charge region depend on the applied potential. Figure 7a shows the plot of capacitance versus potential as obtained through sweeping the potential in the range from 1 to -1.5V/SCE at a constant frequency (1kHz) in D&I conditions. It is observed that the capacitance in the range from 1 to -0.9V/SCE remains approximately constant which is attributed to

a depletion layer. Details which present inset of figure 7a show that space charge capacitance C_{sc} is higher in the dark rather than in illumination. This behavior is concern to charge and discharge of capacitance which we consider this kind of capacitor like Schottky junction in our previous work[20]. The value of C_{sc} is in the range of 1-3 μF.cm^{-2}. It is important to mention that the capacity of the C_H is in series with the C_{sc}:

$$1/C_{total} = 1/C_{sc} + 1/C_H \tag{8}$$

In the depletion layer if C_{sc}<<C_H, therefore the C_H can be neglected. So, the Mott-Schottky relation, equation 9, [37] virtually signifies the space charge capacity:

$$1/C_{sc}^2 = 2/\varepsilon\varepsilon_o e N_D \left(E - E_{fb} - kT/e\right) \tag{9}$$

where e, ε_o, ε, k, and N_D are the elementary charge, the permittivity of free space, the dielectric constant of the semiconductor, the Boltzman constant and the carrier density, respectively. The positive slope of Mott–Schottky plots in the depletion region, figure 7b, show that the CdS thin film is n-type semiconductor[32]. The flat band potential can be determined from the intercept on the E axis. The values of the E_{fb} are -0.916 and -0.976V/SCE in the dark and illumination conditions, respectively. The value of E_{fb} obtained from the Mott-Schottky plot in the dark is approximately close to that of value obtained by *LSV* measurements (at about -0.8V/SCE). Also, according to figure 7b the E_{fb} is shifted cathodically (60 mV) when the ITO/CdS electrode is illuminated. It has been

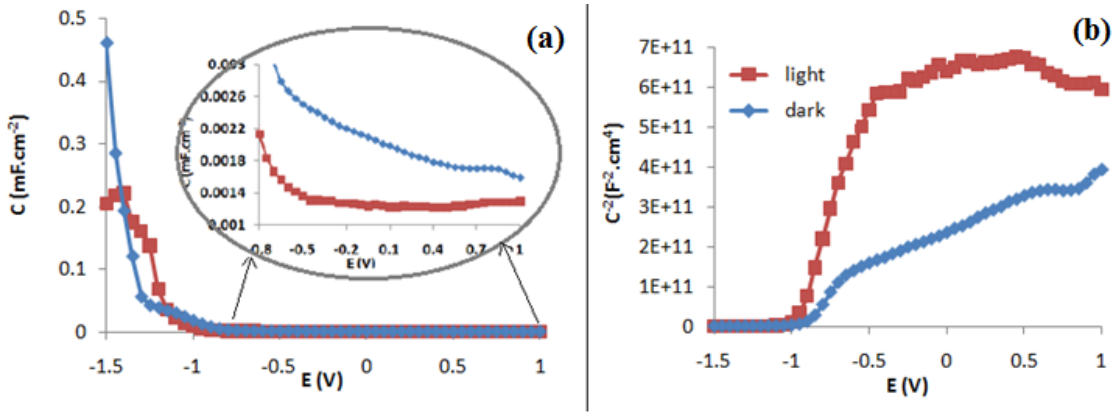

Figure 7. (a) Capacitance-Potential and its insert curves in the depletion region and (b) Mott-Schottky plot of ITO/CdS electrode in the 0.1 M NaOH solution in dark and illumination, in 1 kHz frequency and S.R=50 mV/s.

reported[38] that the cathodic shift is related to the trapping of majority carriers (electrons) in the surface states. So the rate of recombination of electron-hole increases in the surface states due to trapped electrons in this area, this process competes with electrons transferring to the *CB*. Consequently, the accumulation of the electrons in the space charge region occurs in high negative potentials and the space charge capacitance increases. The Q_{ss} is calculated[32] from the corresponding change of E_{fb} using:

$$Q_{ss} = C_H [E_{fb(light)} - E_{fb(dark)}] \tag{10}$$

By inserting Q_{ss} into following relation $N_{ss} = Q_{ss}/e$, electron density N_{ss} could be estimated. By assuming $C_H \approx 10^{-5}$ μF.cm^{-2} and the difference of E_{fb} in D&I conditions is 0.06 V, one obtains 6×10^{-7} C.cm^{-2} and 3.75×10^{12} cm^{-2} for Q_{ss} and N_{ss}, respectively. From the slope of the Mott–Schottky plot, the values of charge carrier density N_D are 1.95×10^{19} and 9.77×10^{18} cm^{-3} in D&I conditions, respectively. The smaller value of N_D under illumination relates to the trapping of some of the charge carriers in the surface states. Nonlinear or segmented Mott–Schottky plot in the dark is related to inhomogeneous donor distribution[39]. Deviation from linearity occurs at about -0.7V/SCE which is confirmed by *LSV* studies. The value of L_D is calculated by the following relation[32]:

$$L_D = \left(\frac{\varepsilon \varepsilon_\circ kT}{2e^2 N_D} \right)^{1/2} \tag{11}$$

Estimated values of E_{fb}, L_D and N_D are listed in table 1. The L_D is inversely proportional to the $(N_D)^{1/2}$ but directly proportional to the thickness of the depletion layer. The large value of L_D under illumination condition is due to the charge separation (*e* and *h*) that happens more effectively with respect to that in the dark condition[32].

Table 1. The semiconductor parameters for n–type CdS thin film

Condition	E_{fb}(V/SCE)	N_D (cm^{-3})	L_D (cm)
Light	-0.976	1.29×10^{17}	6.91×10^{-6}
Dark	-0.916	3.21×10^{17}	4.38×10^{-6}

Consequently, the extracted results from all the electrochemical methods can be summarized in the energy diagram of ITO/CdS thin film, figure 8.

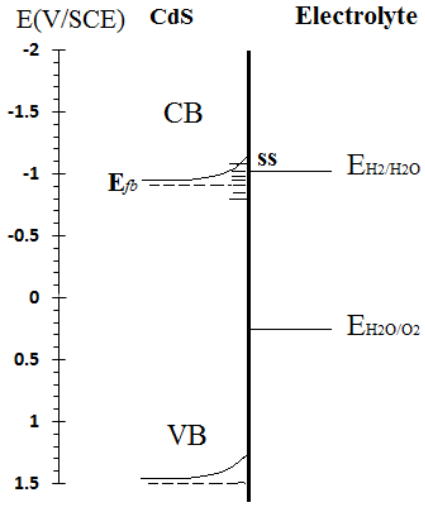

Figure 8. Position of energy bands and Fermi level at the surface of CdS thin film in 0.1 M NaOH solution (pH=13).

3.7. Electrochemical Impedance Spectroscopy

The *EIS* method is used to investigate the charge transfer mechanism in ITO/CdS thin film in the depletion region. Typical Nyquist and Bode plots of ITO/CdS thin film are presented in figures 9a,b&c in 0.1 M NaOH at different potentials. The Nyquist plots consist of two depressed and merged semicircles. All plots were fitted by an equivalent electrical circuit. Several models of circuits were attempted to fit these experimental data. The best fit is achieved with the equivalent circuit presented in figure 9d. In the high frequency, R_s is related to solution resistance. The value of phase is about 20 degree in the Bode-Phase spectra which shows clearly diffusion of electrolyte to

the passive film at high frequencies [40]. In the intermediate frequencies squashed semicircles are observed consisting of two overlapped processes. First time constant $R_{ct}C_{sc}$ shows charge transfer resistance R_{ct} parallel to space charge capacitance C_{sc}. It is observed that at negative potential Bode-Phase spectra are similar to each other in high frequencies (in figure 9c) related to $R_{ct}C_{sc}$ is approximately unchangeable via the distribution of potentials. This behavior is shown being constant of C_{sc} in the depletion region, figure 9c. It is illustrated that R_{ct} is smaller under illumination with respect to the dark at the same potential [21]. As a result of the photo-induced generation of charge carriers the R_{ct} drastically decreases upon illumination[18].

In low frequency region the second time constant changes with variation of potential which it might correspond to the contribution of surface states. The probability of electron-hole recombination

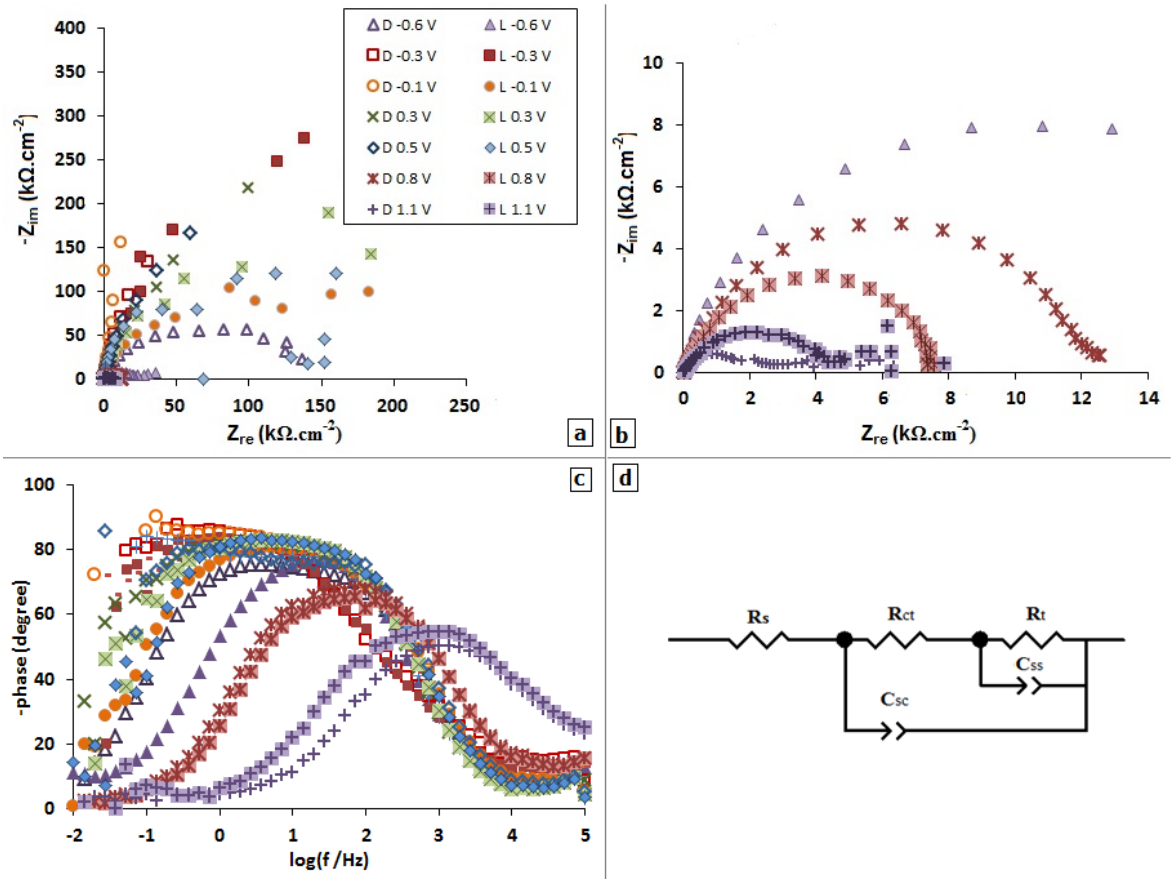

Figure 9. (a) Original and (b) zoomed structure of Nyquist plots, (c) Bode-Phase spectra and (d) equivalent circuit of CdS thin film at different applied potentials in 0.1M NaOH in dark (D) and light (L) conditions.

increases and the recombination resistance R_t decreases when the charge carriers trap in the surface states capacitance C_{ss}. Under these conditions, a large semicircle in the lower frequency regions indicates the low R_t [40]. In figure 9b, the values of phase in Bode-Phase spectra is about 90 degree which show the capacitance behavior of CdS film at the potentials at around open circuit potential (-0.5V/SCE), such as -0.3 and -0.1 V/SCE in the dark. At these potentials the charge transfer or recombination phenomena are small, so electrons conserve in the capacitors. At potentials more than 0.8 V/SCE, R_{ct} decreases remarkably and the second time constant declines. It is due to depletion of surface states from electrons and electrons transfer from H_2O to *VB* of CdS thin film. These results are confirmed by *CV* plots. In the other word after a certain potential holes are injected directly from *VB* into the H_2O giving rise to currents.

4. Conclusions

Here we consider on electrodeposition of CdS film on the ITO. Then the photo-properties of ITO/CdS thin film were investigated by employing the quick, repeatable and simple techniques of electrochemistry. By *CV* method, it is shown the value of band gap is 2.3 eV that it is close to obtained by spectroscopic method (2.25 eV) and there is a direct correlation between two methods. Also, the *LSV*, *CV* and Mott-Schottky plots of the CdS thin film under both dark and illumination conditions indicate that this film behaves as n-type electrode and confirm the presence of surface states in CdS. Also the DOS of CdS thin film is determined by the order of 10^{18} $eV^{-1}.cm^{-2}$ by *CV* technique. From impedance plots the equivalent electrical circuit of transport mechanism is determined at the potentials selected the depletion region. The Nyquist plots indicate that R_{ct} decreases under illumination. The values of E_{fb}, N_D and L_D are obtained -0.916V/SCE, $3.21\times10^{17}cm^{-3}$ and 4.38×10^{-6}cm by Mott-Schottky plot in the dark condition. The difference between the calculated

values of E_{fb}, N_D and L_D in the dark and under illumination condition is shown that the majority charge carriers trapped in the surface state that exhibits the increase in the recombination of holes.

References

1 A. B. Ellis, S. W. Kaiser, M. S. Wrighton, *Journal of the American Chemical Society* **1976**, *98*, 6855-6866.

2 B. R. Karas, A. B. Ellis, *Journal of the American Chemical Society* **1980**, *102*, 968-980.

3 S. Rengaraj, A. Ferancova, S. Jee, S. Venkataraj, Y. Kim, J. Labuda, M. Sillanpää, *Electrochimica Acta* **2010**, *56*, 501-509.

4 P. Bansal, N. Jaggi, S. K. Rohilla, *Research Journal of Chemical Sciences* **2012**, *2*, 69-71.

5 J. Y. Choi, K.-J. Kim, J.-B. Yoo, D. Kim, *Solar energy* **1998**, *64*, 41-47.

6 K. S. Ojha, R. L. Srivastava, *Chalcogenide Letters* **2013**, *10*, 1-10.

7 I. Sisman, M. Alanyalioglu, Ü. Demir, *The Journal of Physical Chemistry C* **2007**, *111*, 2670-2674.

8 S. N. Inamdar, P. P. Ingole, S. K. Haram, *ChemPhysChem* **2008**, *9*, 2574-2579.

9 T. Berger, T. Lana-Villarreal, D. Monllor-Satoca, R. Gomez, *The Journal of Physical Chemistry C* **2007**, *111*, 9936-9942.

10 W.-J. Chun, A. Ishikawa, H. Fujisawa, T. Takata, J. N. Kondo, M. Hara, M. Kawai, Y. Matsumoto, K. Domen, *The Journal of Physical Chemistry B* **2003**, *107*, 1798-1803.

11 F. Fabregat-Santiago, I. Mora-Seró, G. Garcia-Belmonte, J. Bisquert, *The Journal of Physical Chemistry B* **2003**, *107*, 758-768.

12 S. K. Haram, B. M. Quinn, A. J. Bard, *Journal of the American Chemical Society* **2001**, *123*, 8860-8861.

13 F. Koffyberg, F. Benko, *Journal of Applied Physics* **1982**, *53*, 1173-1177.

14 D. Nesheva, S. Rashev, *Thin Solid Films* **1990**, *189*, 1-7.

15 J. Bisquert, *Physical Chemistry Chemical Physics* **2003**, *5*, 5360-5364.

16 F. Fabregat-Santiago, H. Randriamahazaka, A. Zaban, J. Garcia-Canadas, G. Garcia-Belmonte, J. Bisquert, *Physical Chemistry Chemical Physics* **2006**, *8*, 1827-1833.

17 A. S. Bondarenko, G. A. Ragoisha, *Journal of Solid State Electrochemistry* **2005**, *9*, 845-849.

18 A. H. A. Tinuemans, T. P. M. Koster, A. Mackor, J. Schoonman, *Berichte der Bunsengesellschaft für physikalische Chemie* **1986**, *90*, 390-394.

19 I. Abayev, A. Zaban, F. Fabregat-Santiago, J. Bisquert, *physica status solidi (a)* **2003**, *196*, R4-R6.

20 A. Heidaripour, M. Jafarian, F. Gobal, M. Mahjani, S. Miandari, *Journal of Applied Physics* **2014**, *116*, 034906.

21 S. Miandari, M. Jafarian, M. G. Mahjani, A. Heidaripour, *Bulletin of the Chemical Society of Japan* **2015**, *88*, In press 10.1246/bcsj.20140257.

22 C.-Y. Yeh, Z. Lu, S. Froyen, A. Zunger, *Physical Review B* **1992**, *46*, 10086.

23 C. Martínez-Alonso, C. A. Rodríguez-Castañeda, P. Moreno-Romero, C. Coria-Monroy, H. Hu, *International Journal of Photoenergy* **2014**, *2014*.

24 A. Monshi, M. R. Foroughi, M. R. Monshi, *World Journal of Nano Science and Engineering* **2012**, *2*, 154.

25 Y. J. Yang, L. Y. He, Q. F. Zhang, *Electrochemistry communications* **2005**, *7*, 361-364.

26 H. P. Klug, L. E. Alexander, *X-Ray Diffraction Procedures: For Polycrystalline and Amorphous Materials, 2nd Edition, ISBN 0-471-49369-4. Wiley-VCH,* **1974**, *1*.

27 J. Dharma, A. Pisal, C. Shelton, *Application Note* **2009**.

28 F. Xu, J. Benavides, X. Ma, S. G. Cloutier, *Journal of Nanotechnology* **2012**, *2012*.

29 M. Tejos, B. G. Rolón, R. Del Rio, G. Cabello, *Materials Science in Semiconductor Processing* **2008**, *11*, 94-99.

30 N. Ghobadi, *International Nano Letters* **2013**, *3*, 1-4.

31 V. Srikant, D. Clarke, *Journal of applied physics* **1997**, *81*, 6357-6364.

32 R. Memming, *Semiconductor electrochemistry*. Editor, John Wiley & Sons, Germany, **2001,**pp 87-89, 105, 107-109, 166, 190, 194.

33 T. Lopes, L. Andrade, H. A. Ribeiro, A. Mendes, *international journal of hydrogen energy* **2010**, *35*, 11601-11608.

34 J. B. Allen, R. F. Larry, *Department of Chemistry and Biochemistry University of Texas at Austin, John Wiley & Sons, Inc* **2001**.

35 I. Abayev, A. Zaban, V. G. Kytin, A. A. Danilin, G. Garcia-Belmonte, J. Bisquert, *Journal of Solid State Electrochemistry* **2007**, *11*, 647-653.

36 J. Bisquert, F. Fabregat-Santiago, I. Mora-Seró, G. Garcia-Belmonte, E. M. Barea, E. Palomares, *Inorganica Chimica Acta* **2008**, *361*, 684-698.

37 J.-B. Lee, S.-W. Kim, *Materials chemistry and physics* **2007**, *104*, 98-104.

38 K. Gelderman, L. Lee, S. Donne, *Journal of chemical education* **2007**, *84*, 685-688.

39 L. Hamadou, A. Kadri, N. Benbrahim, *Applied surface science* **2005**, *252*, 1510-1519.

40 Q. Wang, J.-E. Moser, M. Grätzel, *The Journal of Physical Chemistry B* **2005**, *109*, 14945-14953.

BCSJ Revised December 2014
The Chemical Society of Japan

Electrochemical determination of CdS band edges and semiconducting parameters

Somaieh Miandari,[1] Majid Jafarian*,[1] Mohammad Ghasem Mahjani,[1] Fereydoon Gobal,[2] and Ashraf Heidaripour[1]

Summery

CdS thin film was deposited on the ITO by chronoamperometry method. Any sheet with a hexagonal structure composed of enormous CdS nanoparticles. Photo-properties and energy diagram of ITO/CdS thin film were characterized by electrochemical techniques such as cyclic voltammetry, linear sweep voltammetry, Mott-Schottky and electrochemical impedance spectroscopy.